Pipeline steel fracture during single edge notched testing using the FEM

[1*]Turbadrakh Chuluunbat, [2]Cheng Lu, and [3]Andrii Kostryzhev

[1] Science and Engineering Department, Mandakh University, Mongolia
[2,3] School of Material, Mechanics and Mechatronic, University of Wollongong, Northfields Ave, Wollongong, NSW 2522, Australia,

[1] turbadrakh@mandakh.mn, [2] cheng@uow.edu.mn, [3] andrii@uow.edu.mn

Abstract: In this paper, fracture initiation and propagation was studied using the Finite Element Modelling (FEM) analysis during single edge notched testing (SENT) of pipeline steel. The Gurson-Tvergaard-Needleman (GTN) constitutive model has been used to simulate the growth of voids during deformation of pipeline steel. FEM simulations confirmed that the fracture was initiated between the yield point and the peak load point on the load-displacement curve for both SENT test, which is in good agreement with the observations from the acoustic emission monitoring.

Keywords: SENT testing, pipeline steel, fracture simulation, AE

Introduction

In the pipeline industry, there is a significant issue to prevent the fracture of pipeline so it is basically demonstrated in terms of fracture initiation and fracture propagation of pipeline. The fracture initiation occurs due to manufacturing defect, design error, and mechanical damages, such as notch, crack, dent, and corrosion, and it reaches a critical defect length or a certain stress level and start to propagate [1, 2] . Once the fracture initiates, it may propagate for long distances in either fully brittle or fully ductile modes, and in theory, could propagate continuously unless arrested by crack arrestors and in practice, could stop itself by certain condition.

Pipelines can be subjected to severe deformations and local defects resulting from bending generated by ground/soil movement or washout during installation and operation, and biaxial loading originating from longitudinal straining and internal pressure [1, 2]. The static fracture toughness of pipeline steel can be obtained from a different type of fracture test, such as a SENT test [3]. Therefore, one of the representative specimens used to evaluate the fracture characteristics of the pipeline was designed to be compatible with a SENT test.

The fracture toughness data obtained from a SENT test can be more suitable for fracture predictions of pressurized pipelines and cylindrical vessels than data obtained from notched fracture specimens under bending and impact loading [4].
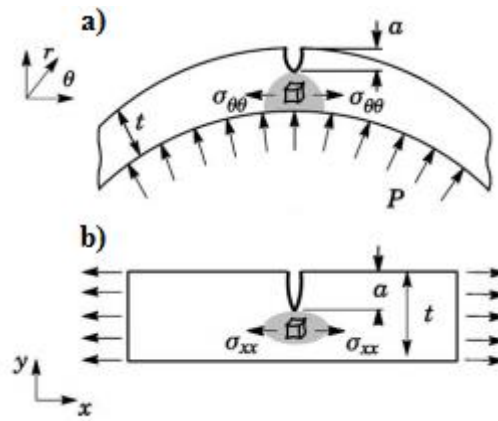
Figure.1 (a) Schematic loading condition for a pressured pipe; (b) SENT test specimen [4].

This is because a SENT test specimen notch resembles surface cracks in pipes more closely, and generates a similar stress field at the crack tip (Figure.1).

The ductile crack growth of the line pipe steels at ambient temperature proceeds via the nucleation, growth and coalescence of micro-voids. As the specimen is loaded, the local strain and stress at the crack tip become sufficient to cause nucleation of voids. These voids grow as the crack blunts, and link with the main crack [3] . The Gurson-Tvergaard-Needleman (GTN) constitutive model has recently become increasingly popular to simulate the growth of voids during deformation [5-8].

In regarding to fracture propagation control, it needs to determine ductile and brittle fracture point. Traditionally, it is assumed that fracture initiates at maximum load during SENT. However, FEM simulations show that the fracture is initiated before or after the load attains its maximum value.

In the present study, finite element simulation of SENT testing was studied to investigate fracture initiation and growth of pipeline steel. Three-dimensional fracture simulations of SENT test has been carried out using the commercial FEM software. These simulations provide a better understanding of the fracture and plastic deformation of the small scale specimen.

FEM simulation

Finite element model
In the present study, the commercial FEM software "ANSYS/LS-DYNA" with dynamic explicit scheme was used to simulate the SENT test [9]. FEM model utilizing eight-node hexahedral elements for the SENT test is employed. The simulation model is shown in Figure 2. The total number of elements and nodes in the simulations are listed in Table 1.

Table 1. The total number of elements and nodes.

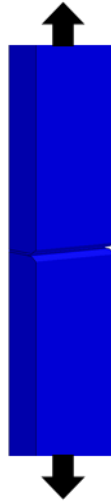|	Number of elements	Numbers of nodes
Simulation of SENT test	129640	140794

Figure 2. A scheme of SENT specimen used in finite element simulation.

The finite element analysis of the SENT specimen was performed using the mesh size of 0.2 mm around the notch area. A constant displacement rate of 20 mm/min was applied in the simulation. The simulation parameters are shown in Table 2. The constant parameters (q_1,q_2) in Gurson-Tvergaard yield function is presented by Tveergard have been applied by many studies for the ductile fracture.

Table 2. GTN parameters used in the simulation.

| GTN parameters	f	f_f	f_c	ε_n	s_n	q_1	q_2
Value	0.000125	0.06	0.0055	0.3	0.1	1.5	1

Test Material

The material used in this experimental work was API-X70 pipeline steel. The specimens were prepared from a 14.1 mm thickness and 106.8 mm diameter pipeline steel. The material composition is given in Table 3.

Table 3. Material composition of the X70 pipeline steel tested.

C	Mn	Si	Nb	Ti	V	Ni	Cr
0.0499	1.56	0.238	0.0576	0.0088	0.0256	0.214	0.028
Cu	Mo	Al	Ca	N	S	P	B
0.163	0.148	0.035	0.0015	0.0036	0.0014	0.0059	0.0001

The fracture toughness obtained using SENT specimens has been recommended by DNV-OS-F101 [10] and DNV-RP-F108 [11]. Recently, a British Standard for the SENT test method has been developed based on DNV-RP-F108. However, the toughness value obtained from the SENT test should be correctly applied to full-scale pipe components.
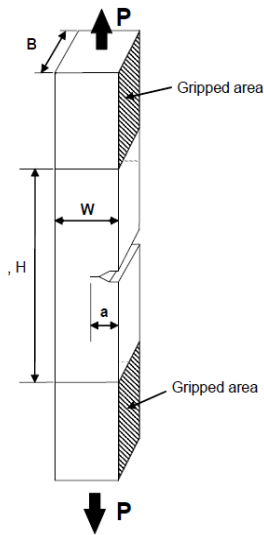
Specimen Geometry:

B- width
W- represent the pipe wall thickness (t)
a-Initial crack length
H- "Day-light between grips"
Requirement of the specimen geometer:
H=10W;
B=2W;
$0.2 \leq a/W \leq 0.5$;
If the reduction on wall thickness due to pipe dimension (D/t) will be more than 15%   (w<0.85 t) the specimen width, B may be reduced but not to less than B≥W:

W (mm)	B (mm)	H (mm)	a (mm)	a/w
6	12	60	2	0.3

Figure 3.The geometry of a single-edge notched specimen used in this work.

Results

Simulated Load-displacement/time curve

Typical load vs displacement/time curve obtained from the FEM simulation is shown in Figure 4.

Similar to the analysis of the experimental results, the load-displacement curve is divided into three regions: I-before the yield point, II-between the yield point and the peak point, and III-after the maximum point till the final fracture. Four points, Points A, B, C and D, are marked in Figure 4..
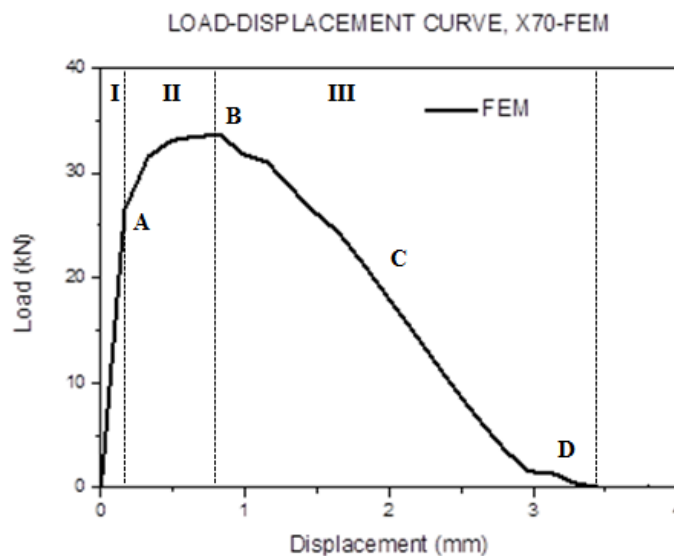

Figure 4. The simulated load-displacement curve, SENT-X70

It can be seen in Figure 4 that the load increases linearly with the displacement in Region I. At point A, which is the yield point, the material at the front of notch area starts to be deformed

plastically.In Region II, from Point A to Point B, the load continuously increases with the displacement. In Region III, the load decreases slightly while the crack propagates and the microviod comfluence exists. In Region III the specimen area reduces and the necking is observed. At Point D, the final separation is observed. FEM simulated load valuesare summarised in Table 4.

Table 4. Summary of simulation results for the SENT specimen.

Load at yield P_{yield}, [N]	Load at crack initiation point $P_{c.i,}$ [N]	Maximum load P_{max}, [N]
24855	33859	34058

Figure 5 compared the specimen geometries predicted in the simulation and recorded by high speed video camera for the four selected points. It can be seen that they are in reasonably good agreement. The determination of fracture initiation plays a very important role in the research of the pipeline fracture control. In this study, a high speed camera has been used to visualize the moment when the fracture initiates.
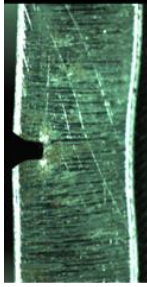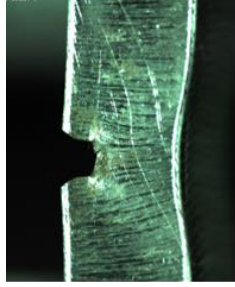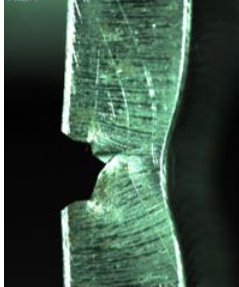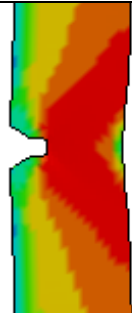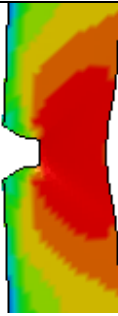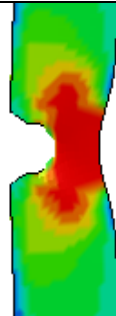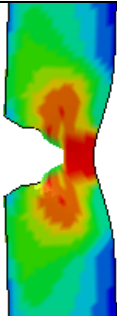

Method	Region I	Region II	Region III	
EXP				
	Selected video shots obtained by high speed camera			
FEM				
	0.33mm (at A point)	0.66 mm (Before B point)	2.15 mm (At C point)	3.24 mm (Before D point)
	Selected effective stress contour			

Figure 5. Fracture process of pipeline steel during SENT testing: Experiment and FEM simulation.

Figure 6 shows the simulated SENT fracture surface and the experimentally tested one. They are in very good agreement. The width extraction and shear fracture area can be observed in both pictures.
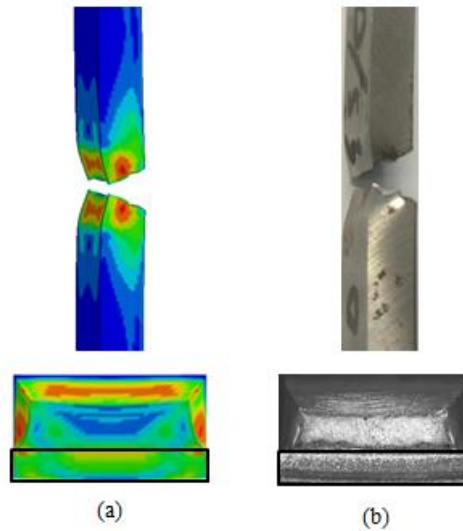
Figure 6. The fractured SENT specimen: Simulated specimen (a); tested specimen (b).

Analysis of crack initiation and propagation

The fracture simulation provides detailed information of the fracture initiation and propagation in a ductile SENT specimen. It has been found that the crack initiates at the displacement of 0.7 mm, which has been marked by a red circle in Figure 7. The effective von Mises stress distribution and fracture morphology corresponding to the crack initiation is shown. It is clear that, at this displacement, a crack nucleates at the notch tip. This simulation result confirms the experimental observations that the fracture initiates prior to the peak load. After the fracture initiation, the load still continues to increase. This is due to the work hardening effect induced by the plastic deformation.
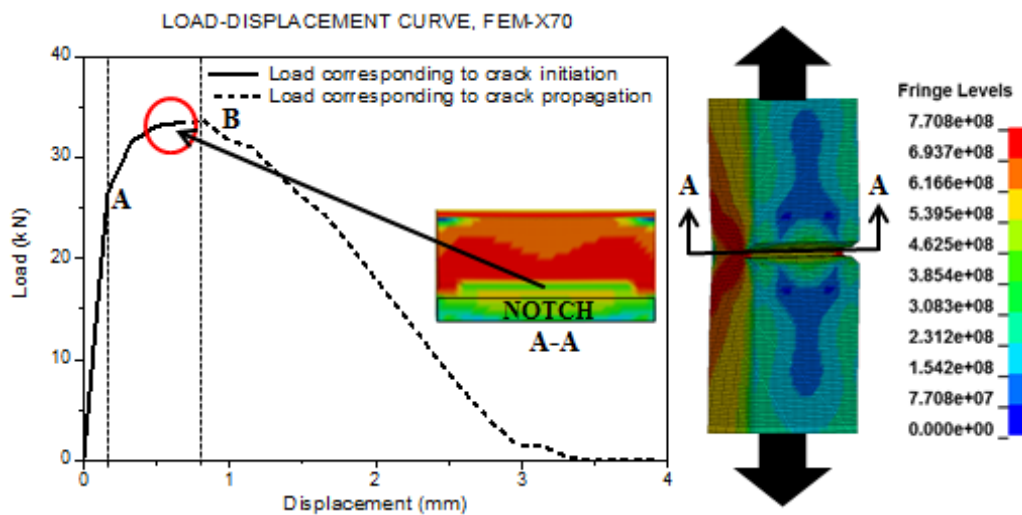

Figure 7. Fracture initiation point determination by FEM simulation for SENT specimen.

In order to analyze, the AE feature before fracture initiation (red circle), Figure 8 has been plotted in the following:
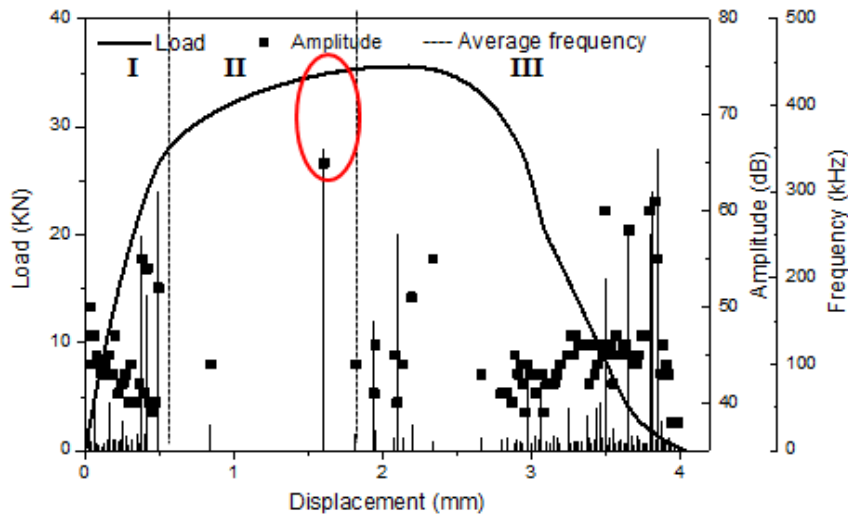
Figure 8. Load-time curves vs AE activity obtained during testing of SENT specimens

Figure 8 shows that there is a rapid change in AE activity; in particular an increase in the AE hit density, signal amplitude and average frequency at Region I. It can be concluded that the rapid change in AE activity in Region II is caused by the fracture initiation. The video data confirms that the fracture initiation is responsible for this event. This finding is similar to some earlier published data. During compact and bending tests of SA333 steel a sudden increase in AE cumulative count and cumulative energy was resulted from crack initiation [13].
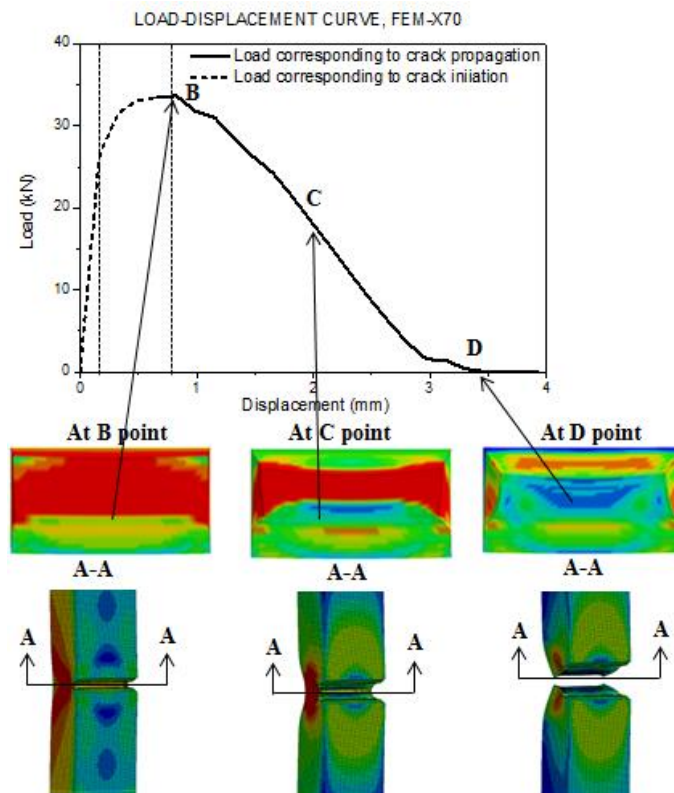

Figure 9. Fracture propagation by the FEM simulation for the SENT specimen.

Figure. 9 shows that the effective von Mises stress distribution and fracture morphology corresponding to the crack propagation from Point B to Point D. It can be seen in Figure 8 that once the fracture is initiated (before B point), the crack propagates rapidly. After Point B the

load decreases slightly. At Point C the fracture area continuously increases and the specimen completely separates at Point D.

Conclusions

It is believed that this work will help to achieve deeper understanding of fracture behavior of pipeline steel and in turn help develop a new pipeline fracture control model.

The research of this paper can be summarized as follows:

1) Three dimensional fracture models based on the finite element method have been developed to simulate the SENT test of the line pipe steel using the Gursen-Tvergaard-Needleman fracture constitutive model.
2) The simulated results are in good agreement with the experimental results in terms of stress distribution and fracture morphology for both SENT tests. The simulated specimen is capable to identify the major characteristics of SENT specimen, such as the fracture tunneling and the shear lip.
3) The fracture initiation can be predicted by the FEM simulation. It has been found that the fracture initiates before the maximum point on the load-displacement curve for both tests.
4) Finite Element Modelling (FEM) simulations confirmed that the fracture was initiated between the yield point and the peak load point on the load-displacement curve for both SENT test, which is in good agreement with the observations from the AE monitoring.

References

1. Rothwell A. B (2000) "Fracture propagation Control for gas pipeline-Past, Present and Future," Pipeline Technology vol. 01, pp. 387-405

2. Anderson T. L. (2005) Fracture mechanics: Fundamentals and Applications. FL: CRC Press

3. Chen Y and Lambert S. (2003) "Analysis of ductile tearing of pipeline -steel in single edge notch tension specimens," *International Journal of Fracture,* vol. 124, pp. 179-199

4. Kofiani K.*, et al.*, (2013). "New calibration method for high and low triaxiality and validation on SENT specimens of API X70," *International Journal of Pressure Vessels and Piping,* vol. 111-112, p p. 187-201

5. Gurson A. L. (1997) "Continuum theory of ductile rupture by void nucleation and growth. Part I. Yeild croteria and flow rules for porous ductile media," Journal of Engineering Materials and Technology, pp. 2-15

6. Tveergaard V. (1981) "Influence of voids on shear band instabilities under plane strain conditions," Acta Materialia, vol. 32, pp. 157-169

7. Tveergaard V., (1984)."Analysis of the cup-cone fracture in a round tensile bar," Acta Metallurgica, vol. 32, pp. 157-169

8. Thibaux P., et al.,(2009) Ductile facture characterization of an X70 steel: Re-interpretation of classical tests using the finite element technique. Calgary

9. LSTC, LS-DYNA (2013) Keyword user's manual (updated manually),

10. DNV-OS-F101, (2000) "Offshore standard-submarine pipeline systems," ed. Norway: Det Norske Veritas,

11. DNV-P-F108, (2006) "Fracture control for pipeline installation methods: Introducing cyclic plastic strain," ed. Norway: Det Norske Veritas

12. Chuluunbat T., et al., (2015) "Investigation of API-X70 line pipe steel fracture during single edge-nothced tensile testing using acoustic emission monitoring," Materials Sceince and Engineering A, vol. 640, pp. 471-479

13. Roy H., et al., (2008) "Acoustic emissions during fracture toughness tests of steels exhibiting varying ductility," Materials Science and Engineering: A, vol. 486, pp. 562-571